



HAL
open science

Combination of 3D Fluorescence/PARAFAC and UV–Vis Absorption for the Characterization of Agricultural Soils from Morocco

Hassan Ba-Haddou, Hicham Hassoun, Salim Foudeil, Abdelmajid El Bakkali, Saadia Ait Lyazidi, Mustapha Haddad, Matthieu Masson, Marina Coquery, Christelle Margoum

► **To cite this version:**

Hassan Ba-Haddou, Hicham Hassoun, Salim Foudeil, Abdelmajid El Bakkali, Saadia Ait Lyazidi, et al.. Combination of 3D Fluorescence/PARAFAC and UV–Vis Absorption for the Characterization of Agricultural Soils from Morocco. *Journal of Fluorescence*, 2022, 32 (6), pp.2141-2149. 10.1007/s10895-022-03011-3. hal-04170117

HAL Id: hal-04170117

<https://hal.inrae.fr/hal-04170117v1>

Submitted on 25 Jul 2023

HAL is a multi-disciplinary open access archive for the deposit and dissemination of scientific research documents, whether they are published or not. The documents may come from teaching and research institutions in France or abroad, or from public or private research centers.

L'archive ouverte pluridisciplinaire **HAL**, est destinée au dépôt et à la diffusion de documents scientifiques de niveau recherche, publiés ou non, émanant des établissements d'enseignement et de recherche français ou étrangers, des laboratoires publics ou privés.

1 Combination of 3D Fluorescence/PARAFAC and UV-Vis Absorption for the characterization of 2 agricultural soils from Morocco

3 Hassan Ba-Haddou^{1,2}, Hicham Hassoun¹, Salim Foudeil¹, Abdelmajid El Bakkali¹, Saadia Ait Lyazidi^{1*},
4 Mustapha Haddad¹, Matthieu Masson², Marina Coquery², Christelle Margoum²

5 ¹Laboratoire de Spectrométrie des Matériaux et Archéomatériaux, URL-CNRST N°7, Faculté des Sciences,
6 Université Moulay Ismail, Meknès, Maroc

7 ²INRAE, UR Riverly, Centre de Lyon-Villeurbanne, F-69625, Villeurbanne, France

8 * Corresponding author: s.aitlyazidi@umi.ac.ma

10 Abstract

11 The present study, combining UV-Visible absorption and 3D fluorescence supported by PARAFAC
12 chemometric analysis, focused on the characterization of soil water extractable organic matter (WEOM) in the
13 zone of Doukkala located near the Atlantic coast of Morocco. The extracts, in water, of a set of 30 samples
14 covering the four main types of agricultural soils in the region (commonly labeled Tirs, Faid, Hamri and R'mel)
15 were investigated. E_2/E_3 and E_4/E_6 absorbance ratios, $S_{275-295}$ and $S_{350-400}$ spectral slopes, along with their
16 ratios S_R , as well as the fluorescence FI and humification HIX indices were calculated and interpreted. In the four
17 soil types these parameters revealed, on the one hand, organic materials of terrigenous origin with a certain
18 biological component, and showed on the other hand that these materials are in similar stages of humification
19 with an important humic character. The 3D fluorescence crossed with PARAFAC chemometrics highlighted the
20 absence of any protein component and revealed the prevalence of the FAs fraction in the OM humic material in
21 all the soils investigated.

22 **Keywords** Morocco . Agricultural Soils . WEOM . UV-Vis. Absorption . Total fluorescence & PARAFAC.

23 Introduction

24 Water extractable organic matter (WEOM), like indigenous dissolved organic matter (DOM) passing a filter pore
25 size of 0.4 – 0.7 μm , is composed of an array of molecules generally reflecting the composition of total soil
26 organic matter [1]. Although it generally comprises < 2% of total soil organic matter, its turnover rate and
27 solubility mean that its role is determinant in many chemical and biological processes in the soil fate [2].
28 Furthermore, while the frontier between DOM and WEOM is not always obvious [3], it is reported that WEOM
29 may likely to contain further material in comparison with indigenous DOM, being thus of larger magnitude [1].
30 Therefore, the properties of WEOM are important indicators of soil quality, namely its physical-chemical and
31 microbial community characteristics [4].

32 Regarding the optical properties, depending on the origin of the OM precursor soil, different fluorescence peaks
33 can be observed on the WEOM fluorescence landscape; they may originate from humic fractions (Humic Acids
34 and Fulvic Acide), protein fractions (mainly tryptophan and tyrosine) or even from persistent contaminants [5,
35 6]. Therefore, WEOM fluorescence landscape is considered as a reliable indicator of the quality of the whole soil
36 organic matter.

37 The geographical area of Doukkala, at the Atlantic coast of Morocco, is known for its important agricultural
38 activity and the diversity of its soils. However, an anterior study of these soils, relating to a 10 years follow-up
39 between 1987 and 1997, revealed an OM depletion [7]. This is why physical-chemical investigations focusing
40 on soils of this highly agricultural region are required. Additionally, during a previous study on the fluorescence
41 analysis of pesticide remains in these soils [6, 8], the WEOM fluorescence was submerging fluorescence signals
42 of pesticides emitting in the same spectral range. This interference made it difficult to discriminate fluorescence
43 signals originating from pesticide remains having a low fluorescence yield.

44 The objective of the present investigation is the analysis of WEOM in the principal soil types in the agricultural
45 zone of Sidi Bennour, in the region of Doukkala. The approach consists in combining UV-Visible absorption and
46 3D fluorescence supported by PARAFAC chemometrics. The goal is to calculate and take mean of the
47 spectroscopic parameters E_2/E_3 and E_4/E_6 absorbance ratios, $S_{275-295}$ and $S_{350-400}$ spectral slopes and slope
48 ratios S_R , as well as fluorescence FI and humification HIX indices. On another side, exploring 3D fluorescence
49 landscapes by visual peak-picking and trough PARAFAC chemometrics will permit the resolution of the
50 underlying fluorescing components.

51 Such optical spectrometric characteristics should make it possible the characterization of the WEOM in these
52 soils, and the discrimination of fluorescence signals originating from emitting organic pollutants persisting in the
53 soil.

54 **Soil Sampling and Analysis**

55 **Soils classification and samples preparation**

56 The investigated soils are classified into four main types according to two previous studies [9, 10]:

57 - Vertisol, commonly labeled Tirs, (52%): deep and clayey soil, with a low permeability, characterized by a high
58 water retention and considered of good productivity.

59 - Slightly evolved, commonly labeled Faid, (17%): deep soil, little to moderately permeable and characterized by
60 a good permeability.

61 - Isohumic, commonly labeled Hamri, (16%): deep to moderately deep soil, with a sandy clay texture and
62 characterized by a good permeability.

63 - Sandy / fersiallitic, commonly labeled R'mel, (13%): sandy in surface and coarse-textured soil, characterized
64 by a high permeability and a low water retention capacity.

65 These soils are neutral to moderately basic [10].

66 Thirty representative soil samples were collected in the province of Sidi Bennour in non-cultivated and non-
67 treated areas neither with pesticides nor with fertilizers. The samples were taken at soil depths ranging from 5 to
68 20 cm, stored in plastic bags and then kept cold.

69 For each soil type, the samples were mixed and shared into several sub-samples of 20g. Avoiding the use of
70 organic solvents, each sub-sample was mixed with 40 ml of water, as an extractor medium, under 1 hour stirring
71 to improve the dissolution of the organic material. The extraction was made at room temperature (at about 20-
72 24°C), protected from light. The water-soil mixture was then stored in dark bottle in the fridge for 24 to 48 h to
73 decant; the final extracts showed pH values in the range 7.5–8.0. As no significant fluorescence intensity
74 difference has been observed between the spectra of filtered through 0.45µm size pores and non-filtered
75 supernatants, the measurements were recorded directly on top-supernatants without filtration. These top-
76 supernatants were transferred into a quartz cell of 1 cm optical path for absorption and fluorescence analyses.

77 **UV-Vis. absorption and fluorescence measurements**

78 The absorption spectra were measured on the top-supernatants using a JASCO UV/VIS/ NIR V-570
79 spectrophotometer; the scans covered the spectral range 200-800 nm.

80 For each type of soil, the average values of the absorbance ratios $\frac{E_2}{E_3} = \frac{A_{250}}{A_{365}}$ and $\frac{E_4}{E_6} = \frac{A_{465}}{A_{665}}$, the slopes
81 $S_{275-295}$ and $S_{350-400}$ as well as slopes ratio $S_R = \frac{S_{275-295}}{S_{350-400}}$ were calculated. A_{250} , A_{365} , A_{465} and A_{665} denote
82 respectively the measured absorbances at 250, 365, 465 and 665 nm wavelengths. The spectral slopes over the
83 intervals 275-295 nm and 350-400 nm were calculated using a linear regression of $\ln(a_\lambda)$, where a_λ is the
84 absorption coefficient calculated in m^{-1} according to the equation $a_\lambda = \frac{2.303 \times A(\lambda)}{l}$, with $A(\lambda)$ and l represent the
85 measured absorbance and the quartz cell thickness (i.e. 0.01 m) [11].

86 The total fluorescence spectra, or excitation-emission matrices also called TEEMs matrices, were measured
87 using a Shimadzu RF-5301PC spectrofluorimeter controlled by LabSolution software. Continuous fluorescence
88 scans were collected between 250 and 700 nm, varying the excitation wavelength from 220 to 550 nm at a 5 nm
89 step. The excitation and emission slits were set at 3 nm (exc.) / 3 nm (em.) or 5 nm (exc.) / 5 nm (em.) depending
90 on the sample.

91 The fluorescence matrix representation adopted in this work is the 2D one where the wavelengths $\lambda_{\text{emission}}$ and
92 $\lambda_{\text{excitation}}$ appear explicitly on the X and Y axes, and the fluorescence intensity is coded by colors ranging from
93 blue to red in rising order of values. The fluorescence maxima correspond to peaks, or foci, identified by their
94 wavelengths coordinates $\lambda_{\text{exc}}/\lambda_{\text{em}}$. Each TEEM requires the concatenation of an average of 57 conventional
95 fluorescence spectra (excitation from 220 to 500 nm at a 5 nm step). LabSolution package crossed with Origin
96 data analysis and graphing software, allowed the representation and manipulation of the measured TEEMs
97 matrices.

99 PARAFAC chemometric analysis

100 The PARAFAC "Parallel Factor Analysis" algorithm is a tool which consists in resolving the measured
 101 fluorescence matrices into individual sub-matrices corresponding to the fluorophores coexisting in the samples
 102 analyzed (supernatants). This chemometric analysis makes it possible to separate the different spectral
 103 contributions associated with the different types of fluorophores in these samples. This means that the positions
 104 $\lambda_{exc}/\lambda_{em}$ of the various underlying signals in a TEEM fluorescence matrix will be determined with a minimal
 105 error; the PARAFAC algorithm is considered by several authors to be a mathematical chromatography. Water
 106 and soil total fluorescence analysis is the analytical method where PARAFAC is being used the most [12 - 14].
 107 The algorithm has been largely elucidated by various authors [15, 16].

108 PARAFAC algorithm principle

109 The algorithm consists in the decomposition of the of the experimental TEEMs data cube, measured on all
 110 samples, into a set of trilinear and residual terms as following.

111 The fluorescence intensity of the sample i for the excitation and emission wavelength pair (k, j) is given by the
 112 equation:

$$X_{i,j,k} = \sum_{f=1}^F a_{i,f} b_{j,f} c_{k,f} + \epsilon_{i,j,k}$$

113 with $i = 1, 2, \dots, I$; $j = 1, 2, \dots, J$ and $k = 1, 2, \dots, K$. I , J and K designate respectively the numbers of samples,
 114 emission wavelengths and excitation wavelengths.

115 $f = 1, 2, \dots, F$. F is the number of components in the model i.e. the presumed number of the fluorophores
 116 coexisting in the samples analyzed.

117 $X_{i,j,k}$ represents the fluorescence intensity of sample i for the pair of excitation and emission wavelengths (k, j) .

118 $a_{i,f}$ represents the fluorescence factor (the concentration times the fluorescence quantum yield); each PARAFAC
 119 component f has I values of a (scores).

120 $b_{j,f}$ represents the intensity of the emission spectrum of the fluorophore f at the emission wavelength j .

121 $c_{k,f}$ represents the value of the absorption spectrum of the fluorophore f at the excitation wavelength K
 122 (proportional to the specific absorption coefficient).

123 $\epsilon_{i,j,k}$ is the residual representing the variability not accounted for by the model, and which the calculation
 124 searches to minimize. This term includes instrumental noises and other non-modellable variations.

125 In this work, the number of components (fluorophores) was varied between 2 and 4. This choice of a reduced
 126 number of components is inspired by the measured TEEMs matrices showing a single fluorescence peak, large
 127 and extended from 370 to 550 nm. The "split-half analysis" method integrated into the algorithm was chosen
 128 during the model validation step. The version of the PARAFAC algorithm used is the online available one [17];
 129 the graphics program used to create the matrices is Matlab.

130 The successful decomposition of a multi-way data system using the PARAFAC algorithm relies on assumptions
 131 about variability, tri-linearity and additivity [15, 16]. In this work, the fluorescence spectra were measured on
 132 samples revealing absorbances at 254 nm lower than 0.5 as can be observed on figure 1; no apparent internal
 133 filter effect was observed. The experimental matrices were corrected from all of the instrumental response, the
 134 internal filter effect and the Raman scattering [16 - 18].

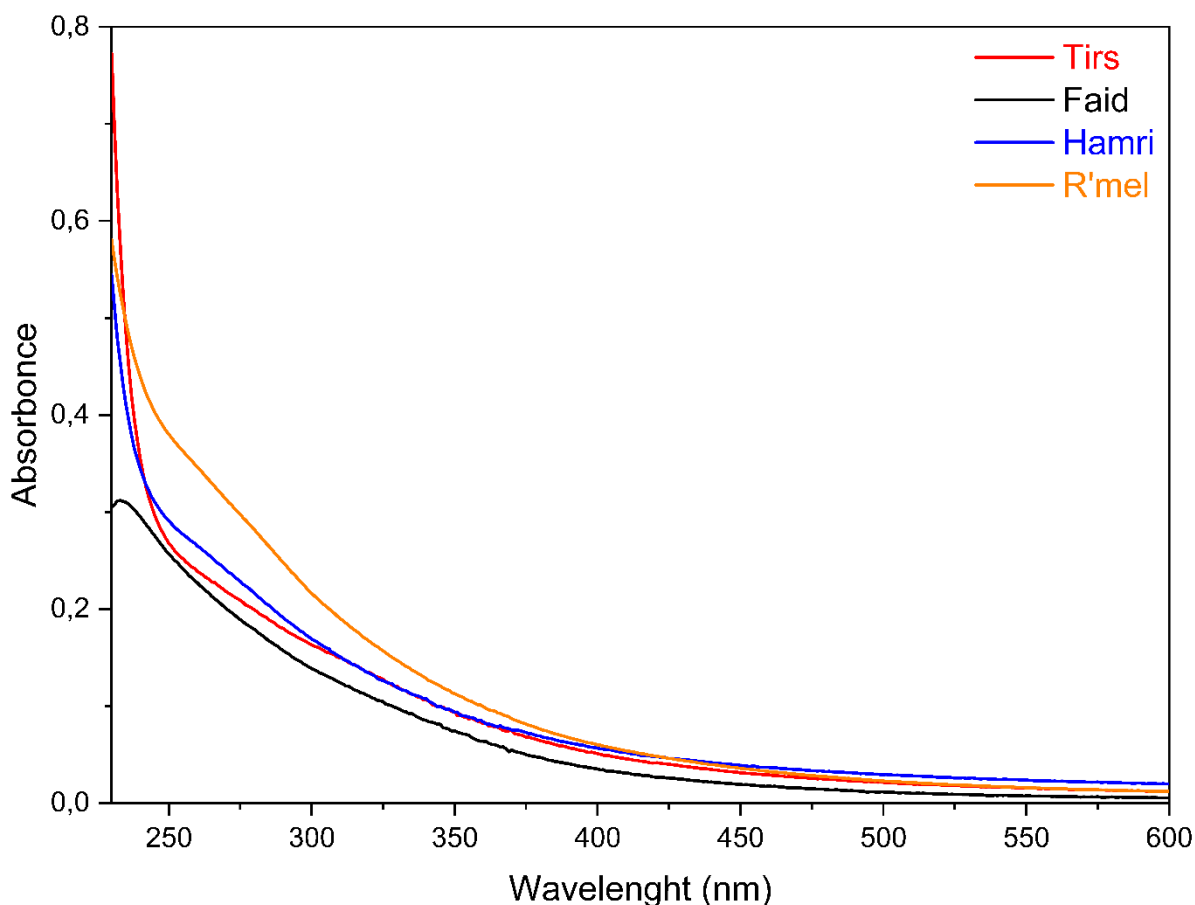
135 Results and discussion

136 UV-Visible Absorption: absorbance and slope ratios

137 In Table 1 are reported, for each type of soil, the average values of the absorbance ratios $\frac{E_2}{E_3} = \frac{A_{250}}{A_{365}}$ and $\frac{E_4}{E_6} =$
 138 $\frac{A_{465}}{A_{665}}$, the slopes $S_{275-295}$ and $S_{350-400}$ as well as the ratios of these slopes $S_R = \frac{S_{275-295}}{S_{350-400}}$.

139 E_4/E_6 ratio is generally related to the degree of condensation and aromaticity of the organic material in the soil
140 [19, 20]; this ratio varies inversely with respect to the degree of condensation / aromaticity. The values found in
141 the case of the four soil types studied, ranging between 3.26 and 4.82, suggest that these soils contain organic
142 materials in close humification stages. The highest value, 4.82, corresponding to the soil Faïd is indicative of an
143 organic material with an aliphatic prevalence of this soil compared to the other ones [20]. This result is also
144 confirmed by the values obtained for E_2/E_3 absorbance ratios varying from 3.77 to 4.33, similar to those
145 reported for other soils [21]. E_2/E_3 ratio is associated with the average weight and molecular size of the organic
146 material contained in the soil [22], and reflects the relative contents of humic acids (HAs) and fulvic acids (FAs).
147 In the present case the values found for E_2/E_3 ratios, all greater than 3.5, indicate organic materials with FAs
148 contents greater than those of HAs [23, 24].

149 Concerning the slopes $S_{275-295}$ and $S_{350-400}$, the average values found for all soil types range respectively in the
150 intervals $0.0101-0.0141 \text{ nm}^{-1}$ and $0.0122-0.0152 \text{ nm}^{-1}$, and are consistent with those reported for other soils
151 [11, 25]. Moreover, the obtained S_R slope ratios, all lower than 1, are reasonably characteristic of terrigenous
152 organic materials generally characterized by $S_{275-295}$ lower than $S_{350-400}$. The difference, of
153 about 20%, observed in S_R between Tirs and R'mel may be probably related to a significant difference in
154 chromophoric DOM (CDOM) in these soils which are respectively the darker and the lighter ones. Furthermore,
155 as slopes and slope ratios are commonly related to the average molecular weight of the organic matter, the
156 similarity of these ratios reveals that the four soil kinds contain organic materials with similar molecular weights
157 [11]. Subsequently, these soils are very likely in similar humification levels as indicated before by E_2/E_3 and
158 E_4/E_6 absorbance ratios.



159

160

Fig. 1 UV-Vis. Absorption spectra measured on top-supernatants of water-soil mixtures.

161

162

163

164

165 **Table 1** Averaged spectroscopic parameters calculated from absorption and fluorescence spectra*

Sol	Tirs	Faid	Hamri	R'mel
E_2/E_3	3.85 ± 0.05	4.33 ± 0.18	3.88 ± 0.03	3.77 ± 0.09
E_4/E_6	3.51 ± 0.11	4.82 ± 0.54	3.26 ± 0.24	3.37 ± 0.18
$S_{275-295}(\text{nm}^{-1})$	0.0101 ± 0.0011	0.0141 ± 0.0009	0.0124 ± 0.0001	0.0126 ± 0.0001
$S_{350-400}(\text{nm}^{-1})$	0.0122 ± 0.0005	0.0152 ± 0.0009	0.0133 ± 0.0001	0.0128 ± 0.0002
S_R	0.8279 ± 0.0450	0.9276 ± 0.0047	0.9323 ± 0.0007	0.9844 ± 0.0331
FI	1.56 ± 0.01	1.52 ± 0.03	1.61 ± 0.01	1.68 ± 0.04
HIX	9.05 ± 0.77	9.26 ± 0.66	12.25 ± 0.83	11.8 ± 0.60

166

167 * More details on the shown parameters are in the text.

168 **Fluorescence: FI and HIX indices**

169 The fluorescence index $FI = \frac{I_{fl}(\lambda_{em}=450 \text{ nm})}{I_{fl}(\lambda_{em}=500 \text{ nm})}$, calculated as the fluorescence intensities ratio at the excitation
 170 wavelength $\lambda_{exc.} = 370 \text{ nm}$, provides information on the origin of the soil organic material; it highlights in
 171 particular the relative importance of the terrigenous material with respect to the microbial biomass one [26].

172 An FI index above 1.8 corresponds to a material with a microbial precursor, while an FI index close to 1.2 is
 173 indicative of a material with a rather terrigenous precursor [27]. In the case of the investigated soils, the FI
 174 indices range in the interval 1.52-1.68. This order of magnitude indicates organic materials from terrigenous
 175 sources with a certain microbial biological component. A similar result was observed in soils from China [28].

176 The humification index HIX calculated as the ratio of fluorescence intensity areas $HIX = \frac{\sum_{\lambda_{em}=435}^{\lambda_{em}=480} I_{fl}}{\sum_{\lambda_{em}=300}^{\lambda_{em}=345} I_{fl}}$, while
 177 excitation wavelength is set at 254 nm, is a parameter positively correlated with the humification / maturation
 178 degree of the soil organic matter [26]. It is often taken as an indicator of DOM variation in agricultural soils [29].
 179 In the present case, the HIX indices vary from 9 to 12. In comparison with the reference intervals given by
 180 various authors [30, 31] the investigated soils can be considered as materials with an important humic character
 181 as a consequence of an advanced maturation stage.

182 **Total fluorescence and PARAFAC chemometrics**

183 **Experimental TEEMs**

184 All soil extracts in water, prepared as described above, were subjected to total fluorescence measurements. In
 185 Figure 2 are presented four examples of the collected raw experimental TEEMs matrices. Likewise, these typical
 186 matrices show a single large fluorescence peak extended, in emission, from 370 to 550 nm. This signal is
 187 attributable to humic substances in the soil organic matter [32, 33]. However, no signal attributable to any
 188 protein fraction has been observed.

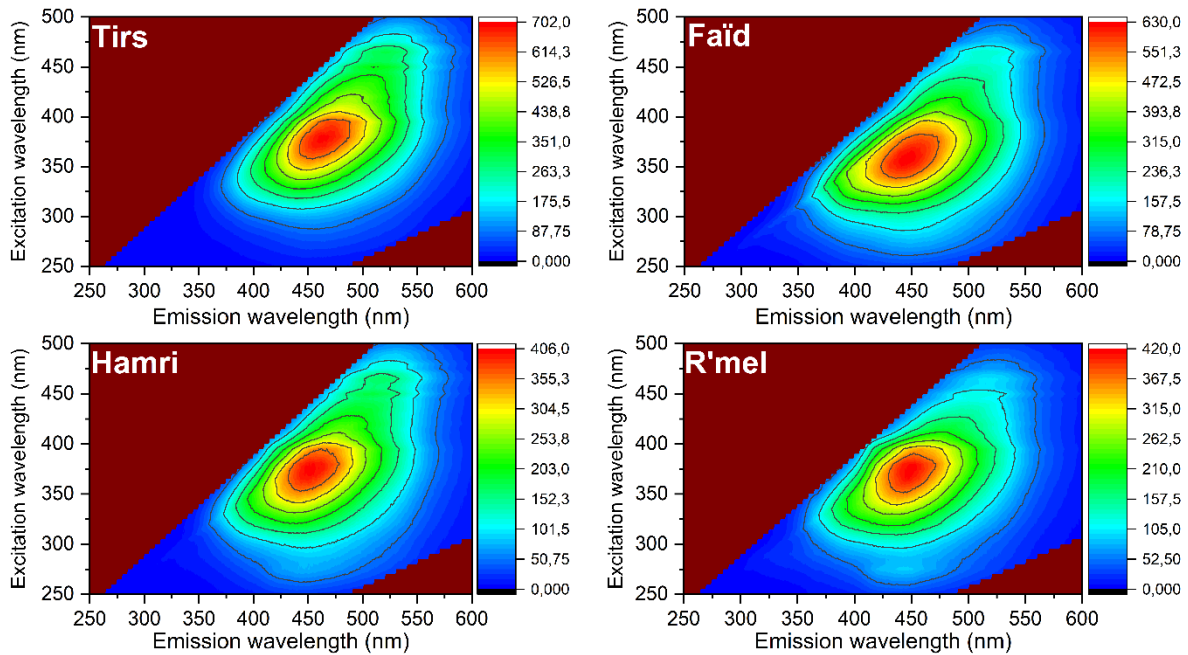


Fig. 2 Examples of experimental total excitation emission matrices (TEEMs).

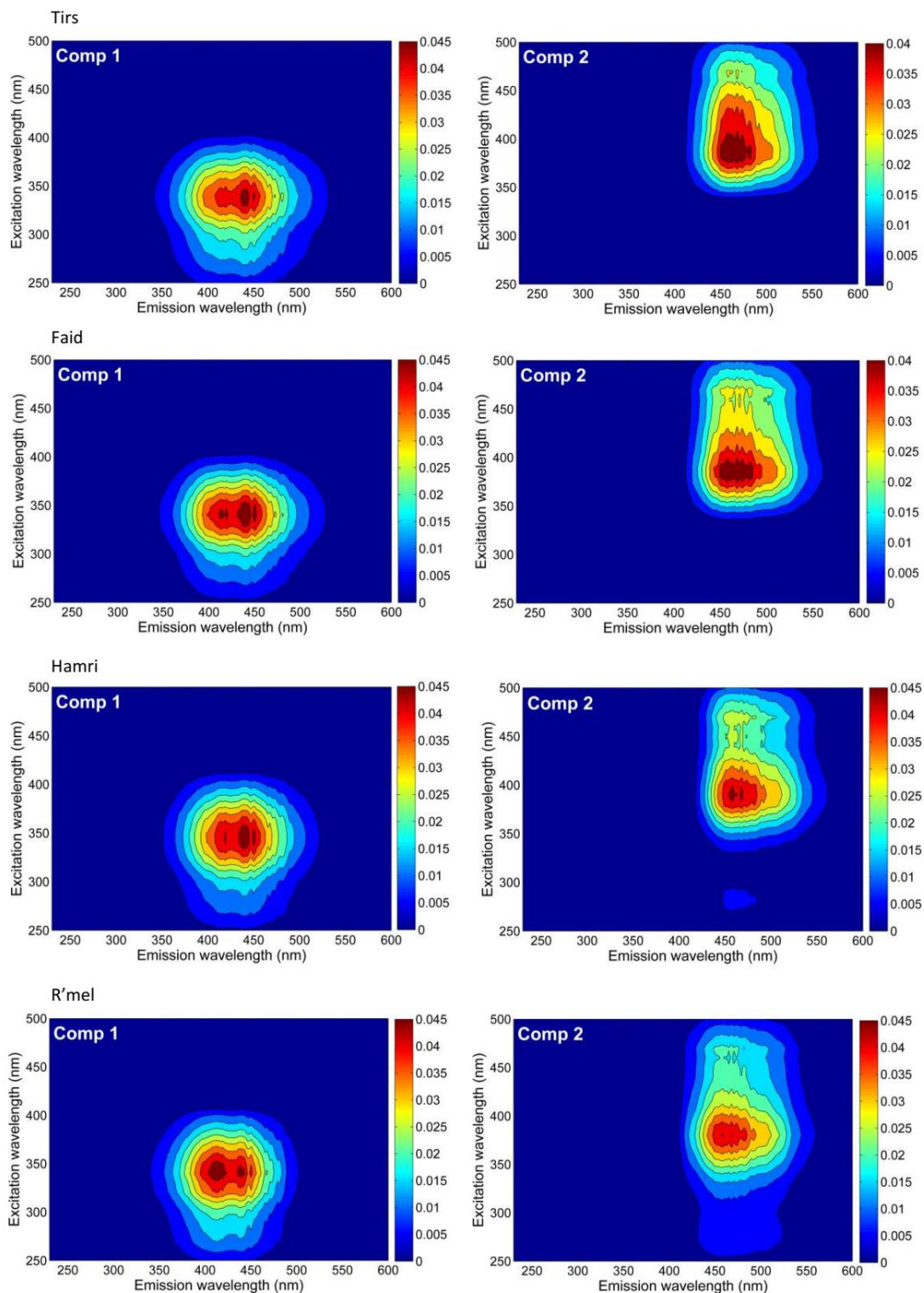
189

190

191 PARAFAC Analysis

192 The PARAFAC chemometric analysis has made it possible to discriminate the fluorescent components
 193 previously overlapping each other in the experimental TEEMs matrices; the procedure is described above. For
 194 all soils, the validated model corresponds to a number of components equal to two, C_1 and C_2 . This model is
 195 entirely consistent with the experimental TEEMs that did not reveal any fluorescence signal outside the spectral
 196 emission range 370-550 nm. Figure 3 shows the individual matrices corresponding to the PARAFAC
 197 components obtained for the four soil types. In all cases the component C_1 appearing around 340exc./442em.
 198 corresponds to the fulvic acid (FAs) fraction while the component C_2 appearing around 385exc./465em.
 199 corresponds to the humic acid (HAs) one of the soils WEOM. Indeed, these fractions are generally observed in
 200 the respective intervals (320-350 nm) exc./ (400-450 nm) em. and (370-390 nm) exc./ (460-500 nm) em. [34,
 201 35].

202 In all soils, the ordering of FAs fraction as component C_1 and HAs fraction as component C_2 is entirely consistent
 203 with the obtained values of E2/E3 absorbance ratios which are greater than 3.5 indicating an organic material
 204 with FAs prevalence. Hence, in the whole of the investigated soils, these findings reflect a dominance of the FAs
 205 fraction with respect to the HAs one [36]. Furthermore, the absence of any PARAFAC component compatible
 206 with a protein fraction, such as tyrosine or tryptophan, reveals highly humified organic materials as previously
 207 highlighted by the HIX humification indices ranging between 9 and 12. The absence of any protein-type
 208 fluorescence signal indicates the absence or, at least, the weakness of proteins microbiological activity in the soil
 209 lands investigated; this is a consequence of the revealed advanced stage of humification. Probably, in the present
 210 soils, the formation of humic substances may be governed by the lignin mechanism putting forward the
 211 hypothesis of the transformation of HAs into FAs [37]. Soil humification means the process leading to the
 212 increasing of the humic material content (namely FAs and HAs); an advanced humification stage may be
 213 associated with an increase in FAs concentration with a decrease in HAs concentration [38]. The formation of
 214 humic substances (HAs, FAs and Humins) is one of the least understood aspects of humus chemistry and one of
 215 the most intriguing.



216

217

218

Fig. 3 Individual total excitation emission matrices of PARAFAC components.
Comp1 and Comp2 designate respectively C1 and C2 components.

219

220 Conclusion

221 The present study focused on the WEOM in a set of thirty agricultural soil samples collected from the zone of
 222 Doukkala in Morocco. The set has covered the four types of agricultural soil (Tirs, Faid, Hamri and R'mel),
 223 while the analysis was performed on the soils extracts in water by means of UV-visible absorption and total
 224 fluorescence combined to PARAFAC chemometrics.

225 E₄/E₆ and E₂/E₃ absorbance ratios, ranging respectively in the intervals 3.26 - 4.82 and 3.77- 4.33, revealed that
226 all soils contain organic materials in similar humification stages, with a predominance of FAs fractions with
227 respect to HAs ones. The average spectral slopes S₂₇₅₋₂₉₅ and S₃₅₀₋₄₀₀ varying respectively in the intervals
228 0.0101-0.0141 nm⁻¹ and 0.0122 - 0.0152 nm⁻¹, with slope ratios S_R lower than 1, are characteristic of terrigenous
229 organic materials. In addition, the FI fluorescence indices found between 1.52 and 1.68 revealed organic
230 materials from terrigenous sources, having some microbial biological component. In parallel, HIX humification
231 indices ranging from 9 to 12 indicated that the soils are in advanced humification stages.

232 3D fluorescence did not detect any protein fraction in the soils WEOM studied, highlighting thus poor fresh
233 organic matter soils. The PARAFAC chemometric analysis, in full agreement with experiments, revealed only
234 two fluorescent components in the humic material with FAs fraction classified as component 1 while HAs one
235 classified as component 2.

236 Consequently, the four types of agricultural soils are compartments in similar humification stages, containing
237 organic materials dominated by FAs fractions and very poorly provided in fresh organic matter.

238 Considering the issue of pesticide remains, the accomplished 3D fluorescence/PARAFAC characterization of the
239 WEOM in the investigated soils will make it possible to discriminate additional fluorescence signals originating
240 from any fluorescent contaminants persisting in the soil.

241 **Authors' contributions.** Hassan Ba-Haddaou: (Experimental investigations, first draft preparation and
242 submission). Hicham Hassoun: (Sampling, material preparation and experimental investigations). Salim Foudeil:
243 (Data collection, first draft preparation and submission). Saadia Ait Lyazidi: (Supervision, methodology, final
244 draft reviewing and project administration). Mustapha Haddad: (Discussion, validation and funding acquisition).
245 Matthieu Masson: (Discussion and validation). Marina Coquery: (Discussion and validation). Christelle
246 Margoum: (Experimental logistics, discussion and validation).

247 All authors read and approved the final manuscript.

248 **Funding** This work has been supported by the Moroccan CNRST (Centre National pour la Recherche
249 Scientifique et Technique) [URL-CNRST N°7].

250 **Data Availability** Not applicable.

251 **Declarations**

252 **Conflicts of interest/Competing interests** The authors declare they have no conflicts of interest and no
253 competing interests.

254 **Ethics Approval** Not applicable as the study does not include any use of animals and humans.

255 **Consent to Participate** All authors consent to participate in the research.

256 **Consent for Publication** All authors consent to participate in the publication of the research.

257 **References**

- 258 1. Zsolnay A (1996) Chapter 4 - Dissolved Humus in Soil Waters. In: Piccolo A, Humic Substances in
259 Terrestrial Ecosystems, Elsevier Science. Pages 171-223. [https://doi.org/10.1016/B978-044481516-](https://doi.org/10.1016/B978-044481516-3/50005-0)
260 [3/50005-0](https://doi.org/10.1016/B978-044481516-3/50005-0)
- 261 2. Chantigny MH, Harrison-Kirk T, Curtin D, Beare M (2014) Temperature and duration of extraction
262 affect the biochemical composition of soil water-extractable organic matter. Soil Biology and
263 Biochemistry 161-166. <https://doi.org/10.1016/j.soilbio.2014.04.011>
- 264 3. Chantigny MH (2003) Dissolved and water-extractable organic matter in soils: a review on the
265 influence of land use and management practices. Geoderma 357-380. [https://doi.org/10.1016/S0016-](https://doi.org/10.1016/S0016-7061(02)00370-1)
266 [7061\(02\)00370-1](https://doi.org/10.1016/S0016-7061(02)00370-1)
- 267 4. Wang W, Zhang W, Majidzadeh H, He C, Shi Q, Kong Q, Yang Z and Wang J (2021) Depletion of Soil
268 Water-Extractable Organic Matter With Long-Term Coverage by Impervious Surfaces. Front Environ
269 Sci 9 : 290. <https://doi.org/10.3389/fenvs.2021.714311>
- 270 5. Sun HY, Koal P, Gerl G, et al (2017) Water-extractable organic matter and its fluorescence fractions in
271 response to minimum tillage and organic farming in a Cambisol. Chem Biol Technol Agric 4, 15.
272 <https://doi.org/10.1186/s40538-017-0097-5>

- 273
274
275
276
277
278
279
280
281
282
283
284
285
286
287
288
289
290
291
292
293
294
295
296
297
298
299
300
301
302
303
304
305
306
307
308
309
310
311
312
313
314
315
316
317
318
319
320
321
322
323
324
325
326
327
328
329
330
331
332
6. Hassoun H, Lamhasni T, Foudeil S, El Bakkali A, Ait Lyazidi S, Haddad M, Choukrad M, and Hnach M (2017) Total fluorescence fingerprinting of pesticides: a reliable approach for continuous monitoring of soils and waters. *J Fluoresc* 27, 1633–1642. <https://doi.org/10.1007/s10895-017-2100-8>
 7. Badraoui M, Agbani M and Soudi B (2000) Evolution de la qualité des sols sous mise en valeur intensive au Maroc. Institut Agronomique et Vétérinaire Hassan II, Rabat, Maroc. <https://agrimaroc.net/intensificationagricole/03-badraoui.pdf> . (accessed on July 15, 2022)
 8. Foudeil S, Hassoun H, Lamhasni T, Ait Lyazidi S, Benyaich F, Haddad M, Choukrad M, Boughdad A, Bounakhla M, Bounouira H, Duarte R M B O, Cachada A, and Duarte A C (2015) Catalogue of total excitation-emission and total synchronous fluorescence maps with synchronous fluorescence spectra of homologated fluorescent pesticides in large use in Morocco: Development of a spectrometric low cost and direct analysis as an alert method in case of massive contamination of soils and waters by fluorescent pesticides. *Environ Sci Pollut Res* 22, 6766–6777. <https://doi.org/10.1007/s11356-014-3807-6>
 9. Billaux P, and Bryssine G, (1967) Les sols du Maroc. In : Congrès de pédologie méditerranéenne: Excursion au Maroc. Cahiers de la Recherche Agronomique. 1, 59-101. https://horizon.documentation.ird.fr/exl-doc/pleins_textes/pleins_textes_5/b_fdi_10-11/13703.pdf. (accessed on July 13, 2022)
 10. Lahbabi A and Anouar K (2009) Rapport de mission « Etude d’Impact sur l’Environnement du projet de Modernisation de l’Agriculture Irriguée dans le bassin de l’Oum Er Rbia ». PROJET UTF/MOR/013/MOR, Assistance technique au projet d’amélioration de la grande irrigation entre L’Organisation des Nations Unies pour l’Alimentation et l’Agriculture (FAO) et le Ministère de l’Agriculture et de la Pêche Maritime Maroc. https://www.academia.edu/47418622/Morocco_Oum_Er_Rbia_Irrigated_Agriculture_Modernization_Project_environmental_report. (accessed on July 15, 2022)
 11. Helms J R, Stubbins A, Ritchie J D, Minor E C, Kieber D J, and Mopper K (2008) Absorption spectral slopes and slope ratios as indicators of molecular weight, source, and photobleaching of chromophoric dissolved organic matter. *Limnol Oceanogr* 53(3): 955–969. <https://doi.org/10.4319/lo.2008.53.3.0955>
 12. Williams C J, Yamashita Y, Wilson H F, Jaffé R, and Xenopoulos M A (2010) Unraveling the role of land use and microbial activity in shaping dissolved organic matter characteristics in stream ecosystems. *Limnol Oceanogr* 55(3): 1159–1171. <https://doi.org/10.4319/lo.2010.55.3.1159>
 13. Shi W, Zhuang W E, Hur J, and Yang L (2021) Monitoring dissolved organic matter in wastewater and drinking water treatments using spectroscopic analysis and ultra-high resolution mass spectrometry. *Water Research* 188: 116406. <https://doi.org/10.1016/j.watres.2020.116406>
 14. Wang YH, Zhang P, He C, Yu JC, Shi Q, Dahlgren RA, Spencer RGM, Yang EB, and Wang JJ (2022) Molecular signatures of soil-derived dissolved organic matter constrained by mineral weathering. *Fundamental research*. 2667-3258. <https://doi.org/10.1016/j.fmre.2022.01.032>
 15. Stedmon C A and Bro R (2008) Characterizing dissolved organic matter fluorescence with parallel factor analysis: a tutorial. *Limnol Oceanogr Methods* 6. <https://doi.org/10.4319/lom.2008.6.572>
 16. Murphy K R, Stedmon C A, Graeber D, and Bro R (2013) Fluorescence spectroscopy and multi-way techniques. *PARAFAC*. *Anal Methods* 5(23): 6557. <https://doi.org/10.1039/c3ay41160e>
 17. Murphy KR, Stedmon CA, Graeber D and R (2013) PARAFAC *Anal Methods*. <http://dreem.openfluor.org/> . (accessed on July 15, 2022)
 18. Murphy K R, Butler K D, Spencer R G M, Stedmon C A, Boehme J R, and Aiken G R (2010) Measurement of Dissolved Organic Matter Fluorescence in Aquatic Environments: An Interlaboratory Comparison. *Environ Sci Technol* 44: 9405–9412. <https://doi.org/10.1021/es102362t>
 19. Chen Y, Senesi N, and Schnitzer M (1977) Information Provided on Humic Substances by E4/E Ratios. *Soil Sci Soc Am J* Vol. 41. <https://doi.org/10.2136/sssaj1977.03615995004100020037x>
 20. Morais D D, Dalmagro H J, Pinto Junior O B, Musis C R, Couto E G, and Johnson M S (2017) Seasonal variation of dissolved organic carbon (DOC) and optical properties of organic matter in different pasture and soybean systems in the State of Mato Grosso. *Ciência e Natura* 39(3): 758-766. <https://doi.org/10.5902/2179460X27649>
 21. Nadi M, Sedaghati E, and Füleky G (2012) Characterization of organic matter content of hungarian agricultural soils. *Acta Agronomica Hungarica* 60(4): 357–366. <https://doi.org/10.1556/AAgr.60.2012.4.6>
 22. Guo M and Chorover J (2003) Transport and fractionation of dissolved organic matter in soil columns. *Soil Science* 168(2): 108-118. <https://doi.org/10.1097/00010694-200302000-00005>
 23. Wang Q, Pang W, Ge S, Yu H, Dai C, Huang X, Li J, and Zhao M (2020) Characteristics of Fluorescence Spectra, UV Spectra, and Specific Growth Rates during the Outbreak of Toxic *Microcystis Aeruginosa* FACHB-905 and Non-Toxic FACHB-469 under Different Nutrient Conditions in a Eutrophic Microcosmic Simulation Device. *Water* 12(8): 2305. <https://doi.org/10.3390/w12082305>

- 333 24. Niloy N M, Haque M M, and Tareq S M (2021) Characterization of dissolved organic matter at urban
334 and industrial rainwater of Bangladesh by fluorescence spectroscopy and EEM-PARAFAC modeling.
335 Environmental Challenges 5: 100250. <https://doi.org/10.1016/j.envc.2021.100250>
- 336 25. Spencer R G M, Butler K D, and Aiken G R (2012) Dissolved organic carbon and chromophoric
337 dissolved organic matter properties of rivers in the USA. Journal of Geophysical Research 117.
338 G03001. <https://doi.org/10.1029/2011JG001928>
- 339 26. Gabor R S, Baker A, McKnight D M, and Miller M P (2014) Fluorescence Indices and Their
340 Interpretation. UCL Cambridge University Press 303-338.
341 <https://doi.org/10.1017/CBO9781139045452.015>
- 342 27. McKnight D M, Boyer E W, Westerhoff P K, Doran P T, Kulbe T, and Andersen D T (2001)
343 Spectrofluorometric characterization of dissolved organic matter for indication of precursor organic
344 material and aromaticity. Limnology and Oceanography 46: 38 – 48.
345 <https://doi.org/10.4319/lo.2001.46.1.0038>
- 346 28. Qin Xq, Yao B, Jin L, Zheng Xz, Ma j, Benedetti M F, Li Y, and Ren Zl (2020) Characterizing Soil
347 Dissolved Organic Matter in Typical Soils from China Using Fluorescence EEM-PARAFAC and UV-
348 Visible Absorption. Aquat Geochem 26: 71-88. <https://doi.org/10.1007/s10498-019-09366-7>
- 349 29. Gao J, Liang C, Shen G, Lv J, Wu H (2017) Spectral characteristics of dissolved organic matter in
350 various agricultural soils throughout China. Chemosphere. 176:108-116.
351 <https://doi.org/10.1016/j.chemosphere.2017.02.104>
- 352 30. Vacher L (2004) Étude par fluorescence des propriétés de la matière organique dissoute dans les
353 systèmes estuariens. Cas des estuaires de la Gironde et de la Seine. PhD thesis, Université Bordeaux 1
- 354 31. Huguet A, Vacher L, Relexans S, Saubusse S, Froidefond J M, and Parlanti E (2009) Properties of
355 fluorescent dissolved organic matter in the Gironde Estuary. Organic Geochemistry 40(6): 706-719.
356 <https://doi.org/10.1016/j.orggeochem.2009.03.002>
- 357 32. Gao J, Liang C, Shen G, Lv J, and Wu H (2017) Spectral characteristics of dissolved organic matter in
358 various agricultural soils throughout China. Chemosphere 176: 108-116.
359 <https://doi.org/10.1016/j.chemosphere.2017.02.104>
- 360 33. Han Z, Xiao M, Yue F, Yi Y, and Mostofa K M G (2021) Seasonal Variations of Dissolved Organic
361 Matter by Fluorescent Analysis in a Typical River Catchment in Northern China. Water 13: 494.
362 <https://doi.org/10.3390/w13040494>
- 363 34. Spencer R G M, Bolton L, and Baker A (2007) Freeze/thaw and pH effects on freshwater dissolved
364 organic matter fluorescence and absorbance properties from a number of UK locations. Water Research
365 41(13): 2941 – 2950. <https://doi.org/10.1016/j.watres.2007.04.012>
- 366 35. Baker A (2001) Fluorescence Excitation-Emission Matrix Characterization of Some Sewage-Impacted
367 Rivers. Environ Sci Technol 35: 948-953. <https://doi.org/10.1021/es000177t>
- 368 36. Minero C, Lauri V, Falletti G, Maurino V, Pelizzetti E, and Vione D (2007) Spectrophotometric
369 characterization of surface lakewater samples: Implications for the quantification of nitrate and the
370 properties of dissolved organic matter. Ann Di Chem 97: 1007-1116.
371 <https://doi.org/10.1002/adic.200790094>
- 372 37. Weber J (2020) definition of soil organic matter. In : Humintech
373 https://www.humintech.com/fileadmin/content_images/agriculture/information/articles_pdf/DEFINITI
374 [ON OF SOIL ORGANIC MATTER.pdf](https://www.humintech.com/fileadmin/content_images/agriculture/information/articles_pdf/DEFINITI). (accessed on July 13, 2022)
- 375 38. Schnitzer M (1967) Humic-fulvic acid relationships in organic soils and humification of the organic
376 matter in these soils. Can J Soil Sci 47(3): 245-250. <https://doi.org/10.4141/cjss67-038>